JOC Article

Nucleic Acid Structural Engineering Using Pyrene-Functionalized 2′-Amino-α-L-LNA Monomers and Abasic Sites

T. Santhosh Kumar,[†] Andreas S. Madsen,[†] Michael E. Østergaard,[‡] Jesper Wengel,*[,†] and Patrick J. Hrdlicka*[,‡]

Nucleic Acid Center, Department of Physics and Chemistry, University of Southern Denmark, 5230 Odense M, Denmark, and Department of Chemistry, University of Idaho, Moscow, Idaho 83844-2343

jwe@ifk.sdu.dk; hrdlicka@uidaho.edu

Received March 14, 2008

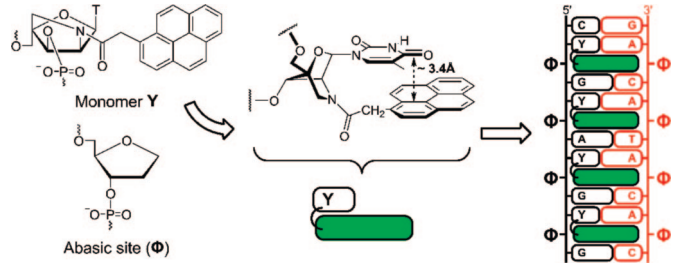

Oligonucleotides (ONs) modified with a 2′-*N*-(pyren-1-yl)acetyl-2′-amino-α-L-LNA thymine monomer **Y** flanked on the 3′-side by an abasic site **Φ** (i.e., **YΦ**-unit) exhibit unprecedented increases in thermal affinity (ΔT_m values) toward target strands containing abasic sites (ΔT_m per **YΦ** unit >+33.0 °C in 9-mer duplexes relative to unmodified ONs). Biophysical studies along with force field calculations suggest that the conformationally locked 2-oxo-5-azabicyclo[2.2.1]heptane skeleton of monomer **Y**, in concert with the short rigid acetyl linker, efficiently forces the thymine and pyrene moieties to adopt an interplanar distance of ∼3.4 Å. This precisely positions the pyrene moiety in the duplex core void formed by abasic sites (**Φ**:**Φ** pair) for optimal $\pi-\pi$ overlap. Duplexes with multiple **YΦ**:**AΦ** units separated by one base pair are tolerated extraordinarily well, as exemplified by a 13-mer duplex containing four separated **YΦ**:**AΦ** units (8 abasic sites distributed over 13 "base pairs"), which exhibit a thermal denaturation temperature of 60.5 °C. The **YΦ** probes display up to 16-fold increases in fluorescence intensity at 380 nm upon hybridization with abasic target strands, whereby self-assembly of these complex architectures can be easily monitored. This study underlines the potential of N2′-functionalized 2′-amino-α-L-LNA as building blocks in nucleic acid based diagnostics and nanomaterial engineering.

Introduction

Hydrogen bonding according to Watson−Crick rules and intrastrand/interstrand base stacking has traditionally been considered the crucial forces ensuring structural integrity of nucleic acid type duplexes.[1] This classical viewpoint has gradually been altered over the past decades as a response to studies on nucleic acids modified with monomers containing nucleobase surrogates. These building blocks loosely fall in two groups: (a) those with surrogates that do not form appreciable hydrogen bonds and are simple hydrocarbons, steric mimics of natural bases, fluorescent bases, and/or rely on interactions between fluorous species for "base pairing",[2−4] or (b) those with surrogates that are capable of forming metal complexes to engage in artificial base pairing.[5,6] Recently, studies have been extended to encompass nucleic acid duplexes modified with non-nucleosidic building blocks carrying nucleobase surrogates.[7] In concert, these studies suggest that nucleobase stacking, hydrophobicity, and hybridization-induced desolvation play important roles in ascertaining integrity of nucleic acid duplexes, while hydrogen bonding is not strictly needed. As an outcome of these investigations, numerous chemical and biological tools have been developed including (a) probes to study mechanism of

[†] University of Southern Denmark.
[‡] University of Idaho.

(1) Saenger, W. *Principles of Nucleic Acid Structure*; Springer-Verlag: New York, 1984.

(2) For reviews, see: (a) Kool, E. T.; Morales, J. C.; Guckian, K. M. *Angew. Chem., Int. Ed.* **2000**, *39*, 990–1009. (b) Kool, E. T. *Acc. Chem. Res.* **2002**, *35*, 936–943.

10.1021/jo800551j CCC: $40.75
Published on Web 08/19/2008

enzymes involved in nucleic acid processing and artificial genetic systems,[8] (b) universal bases for use at ambiguous sites in primers during replication,[9] and (c) fluorescent probes for detection of hybridization to DNA/RNA complements or presence of single nucleotide polymorphisms.[10]

Another outcome of these efforts has been the development of building blocks that detect[11,12] or stabilize abasic sites,[3a,c,i,7e,g,13,14] that is, DNA lesions that can lead to genomic mutations and development of cancers if unrepaired.[15] Abasic sites exert detrimental effects on nucleic acid duplex stability when present opposite of natural nucleobases since base stacking is discontinued.[16,17] Building blocks that contain extended aromatic nucleobase surrogates can occupy the cavity formed by the missing nucleobase moiety and reestablish $\pi-\pi$ stacking in the lesion site.[13] Oligonucleotides (ONs) containing incorporations of *nonnucleosidic* building blocks with phenanthroline,[7g] phenanthrene,[7e] or pyrene[7g] as nucleobase surrogates moderately stabilize target strands containing abasic sites, that is, leading to thermal denaturation temperatures (T_m values) of duplexes with surrogate:abasic site pairs that are 0−8 °C higher than those of the corresponding duplexes with adenine:abasic site pairs. Probes containing incorporations of *nucleosides* modified with fluoroaromatic,[3c] bipyridyl,[3i] or biphenyl nucleobase surrogates[3i] stabilize abasic sites to a similar extent but still yield duplexes that are substantially more unstable than duplexes with native A:T pairs. ONs modified with nucleosides with phenyl- or naphthyl-modified adenine[14] or pyrene[3a,4c] nucleobase surrogates exhibit the largest reported increases in thermal affinity toward strands containing abasic sites (ΔT_m values = +12−20 °C). Duplexes containing these surrogate:abasic site pairs exhibit similar thermal stability as the corresponding duplexes with A:T pairs.[3a,14]

As a result of our continued efforts to explore locked nucleic acids (LNA),[18,19] α-L-LNA[20] and their 2′-amino analogues[21,22] in nucleic acid based therapeutics, diagnostics, and nanomaterial engineering,[23] we have recently investigated different pyrene-functionalized derivatives thereof[4,24] including pyrene-functionalized 2′-amino-α-L-LNA monomers.[25] Incorporation of the latter type of monomers into ONs results in extensive duplex stabilization presumably as a consequence of precise positional control of intercalators in the duplex core. This prompted us to investigate the ability of these monomers to stabilize duplexes containing abasic sites, the results of which are presented in the following.[26]

Results and Discussion

ONs modified with model abasic site (**Φ**),[16] α-L-LNA (**O**),[20] 2′-amino-α-L-LNA (**X**),[22] or 2′-*N*-(pyren-1-yl)acetyl-2′-amino-α-L-LNA (**Y**)[25b] monomers (Scheme 1) were prepared for this study. The corresponding phosphoramidites of 2′-amino-α-L-LNA thymine monomers **X**[22] and **Y**[25b] were synthesized and used for incorporation of **X** and **Y** into ONs as previously described. Phosphoramidites for incorporation of α-L-LNA thymine (**O**)[20] and abasic site (**Φ**) monomers were acquired from commercial sources and used on an automated nucleic acid synthesizer for incorporation of **O** and **Φ** into ONs using

(3) For representative examples, see the following references cited therein: (a) Matray, T. J.; Kool, E. T. *J. Am. Chem. Soc.* **1998**, *120*, 6191–6192. (b) Guckian, K. M.; Ren, R. X.-F.; Chaudhuri, N. C.; Tahmessebi, D. T.; Kool, E. T. *J. Am. Chem. Soc.* **2000**, *122*, 2213–2222. (c) Parsch, J.; Engels, J. W. *Helv. Chim. Acta* **2000**, *83*, 1791–1808. (d) Mathis, G.; Hunziker, J. *Angew. Chem., Int. Ed.* **2002**, *41*, 3203–3205. (e) Singh, I.; Hecker, W.; Prasad, A. K.; Parmar, V. S.; Seitz, O. *Chem. Commun.* **2002**, 500–501. (f) Kubota, M.; Ono, A. *Tetrahedron Lett.* **2004**, *45*, 5755–5758. (g) Matsuda, S.; Romesberg, F. E. *J. Am. Chem. Soc.* **2004**, *126*, 14419–14427. (h) Zahn, A.; Brotschi, C.; Leumann, C. J. *Chem.—Eur. J.* **2005**, *11*, 2125–2129. (i) Brotschi, C.; Mathis, G.; Leumann, C. J. *Chem.—Eur. J.* **2005**, *11*, 1911–1923. (j) Zivkovic, A.; Engels, J. W. *Nucleosides Nucleotides Nucleic Acids* **2005**, *24*, 1023–1027. (k) Hwang, G. T.; Romesberg, F. E. *Nucleic Acids Res.* **2006**, *34*, 2037–2045. (l) Krueger, A. T.; Lu, H.; Lee, A. H. F.; Kool, E. T. *Acc. Chem. Res.* **2007**, *40*, 141–150.

(4) (a) Babu, B. R.; Prasad, A. K.; Trikha, S.; Thorup, N.; Parmar, V. S.; Wengel, J. *J. Chem. Soc. Perkin Trans. 1* **2002**, *2509*, 2519. (b) Raunak, Babu, B. R.; Sørensen, M. D.; Parmar, V. S.; Harrit, N. H.; Wengel, J. *Org. Biomol. Chem* **2004**, *2*, 80–89. (c) Verhagen, C.; Bryld, T.; Raunkær, M.; Vogel, S.; Buchalová, K.; Wengel, J. *Eur. J. Org. Chem.* **2006**, 2538–2548.

(5) For a review, see: Clever, G. H.; Kaul, C.; Carell, T. *Angew. Chem., Int. Ed.* **2007**, *46*, 6226–6236.

(6) For representative examples, see: (a) Weizman, H.; Tor, Y. *J. Am. Chem. Soc.* **2001**, *123*, 3375–3376. (b) Tanaka, K.; Tengeiji, A.; Kato, T.; Toyama, N.; Shionoya, M. *Science* **2003**, *299*, 1212–1213. (c) Zimmermann, N.; Meggers, E.; Schultz, P. G. *Bioorg. Chem.* **2004**, *32*, 13–25. (d) Switzer, C.; Sinha, S.; Kim, P. H.; Heuberger, B. D. *Angew. Chem., Int. Ed.* **2005**, *44*, 1529–1532. (e) Zhang, L.; Meggers, E. *J. Am. Chem. Soc.* **2005**, *127*, 74–75. (f) Tanaka, K.; Clever, G. H.; Takezawa, Y.; Yamada, Y.; Kaul, C.; Shionoya, M.; Carell, T. *Nat. Nanotechnol.* **2006**, *1*, 190–194. (g) Clever, G. H.; Carell, T. *Angew. Chem., Int. Ed.* **2007**, *46*, 250–253.

(7) For representative examples, see: (a) Christensen, U. B.; Pedersen, E. B. *Nucleic Acids Res.* **2002**, *30*, 4918–4925. (b) Yamana, K.; Iwai, T.; Ohtani, Y.; Sata, S.; Nakamura, M.; Nakano, H. *Bioconjugate Chem.* **2002**, *13*, 1266–1273. (c) Malakhov, A. D.; Skorobogatyi, M. V.; Prokhorenko, I. A.; Gontarev, S. V.; Kozhich, D. T.; Stetsenko, D. A.; Stepanova, I. A.; Shenkarev, Z. O.; Berlin, Y. A.; Korshun, V. A. *Eur. J. Org. Chem.* **2004**, *1298*, 1307. (d) Okamoto, A.; Ichiba, T.; Saito, I. *J. Am. Chem. Soc.* **2004**, *126*, 8364–8365. (e) Langenegger, S. M.; Häner, R. *Chem. Biodiversity* **2004**, *1*, 259–264. (f) Kohler, O.; Venkatrao, D.; Jarikote, D. V.; Seitz, O. *ChemBioChem* **2005**, *6*, 69–77. (g) Langenegger, S. M.; Häner, R. *ChemBioChem* **2005**, *6*, 848–851. (h) Kashida, H.; Tanaka, M.; Baba, S.; Sakamoto, T.; Kawai, G.; Asanuma, H.; Komiyama, M. *Chem.—Eur. J.* **2006**, *12*, 777–784. (i) Kashida, H.; Asanuma, H.; Komiyama, M. *Chem. Commun.* **2006**, *2768*, 2770. (j) Malinovski, V. L.; Samian, F.; Häner, R. *Angew. Chem., Int. Ed.* **2007**, *46*, 4464–4467.

(8) Reviewed in refs 2a and: (a) Kool, E. T. *Annu. Rev. Biochem.* **2002**, *71*, 191–219. (b) Henry, A. A.; Romesberg, F. E. *Curr. Opin. Chem. Biol* **2003**, *7*, 727–733. (c) Hirao, I. *Curr. Opin. Chem. Biol.* **2006**, *10*, 622–627.

(9) Loakes, D. *Nucleic Acids Res.* **2001**, *29*, 2437–2447.

(10) Reviewed in: (a) Okamoto, A.; Saito, Y.; Saito, I. *J. Photochem. Photobiol. C* **2005**, *6*, 108–122. (b) Wilson, J. N.; Kool, E. T. *Org. Biomol. Chem.* **2006**, *4*, 4265–4274.

(11) Valis, L.; Amann, N.; Wagenknecht, H.-A. *Org. Biomol. Chem.* **2005**, *3*, 36–38.

(12) Greco, N. J.; Tor, Y. *J. Am. Chem. Soc.* **2005**, *127*, 10784–10785.

(13) Smirnov, S.; Matray, T. J.; Kool, E. T.; Santos, C. I. *Nucleic Acids Res.* **2002**, *30*, 5561–5569.

(14) Nakano, S.; Uotani, Y.; Uenishi, K.; Fujii, M.; Sugimoto, N. *Nucleic Acids Res.* **2005**, *33*, 7111–7119.

(15) Schärer, O. D. *Angew. Chem., Int. Ed.* **2003**, *42*, 2946–2974.

(16) Millican, T. A.; Mock, G. A.; Chauncey, M. A.; Patel, T. P.; Eaton, M. A. W.; Gunning, J.; Cutbush, S. D.; Neidle, S.; Mann, J. *Nucleic Acids Res.* **1984**, *12*, 7435–7453.

(17) Vesnaver, G.; Chang, C-N.; Eisenberg, M.; Grollman, A. P.; Breslauer, K. J. *Proc. Natl. Acad. Sci. U.S.A.* **1989**, *86*, 3614–3618.

(18) Wengel, J. *Acc. Chem. Res.* **1999**, *32*, 301–310.

(19) Petersen, M.; Wengel, J. *Trends Biotechnol.* **2003**, *21*, 74–81.

(20) Sørensen, M. D.; Kværnø, L.; Bryld, T.; Håkansson, A. E.; Verbeure, B.; Gaubert, G.; Herdewijn, P.; Wengel, J. *J. Am. Chem. Soc.* **2002**, *124*, 2164–2176.

(21) Singh, S. K.; Kumar, R.; Wengel, J. *J. Org. Chem.* **1998**, *63*, 10035–10039.

(22) Kumar, T. S.; Madsen, A. S.; Wengel, J.; Hrdlicka, P. J. *J. Org. Chem.* **2006**, *71*, 4188–4201.

(23) Wengel, J. *Org. Biomol. Chem.* **2004**, *2*, 277–280.

(24) (a) Sørensen, M. D.; Petersen, M.; Wengel, J. *Chem. Commun.* **2003**, 2130–2131. (b) Hrdlicka, P. J.; Babu, B. R.; Sørensen, M. D.; Wengel, J. *Chem. Commun.* **2004**, 1478–1479. (c) Hrdlicka, P. J.; Babu, B. R.; Sørensen, M. D.; Harrit, N.; Wengel, J. *J. Am. Chem. Soc.* **2005**, *127*, 13293–13299. (d) Lindegaard, D.; Babu, B. R.; Wengel, J. *Nucleosides Nucleotides Nucleic Acids* **2005**, *24*, 679–681. (e) Umemoto, T.; Hrdlicka, P. J.; Babu, B. R.; Wengel, J. *ChemBioChem* **2007**, *8*, 2240–2248. (f) Lindegaard, D.; Madsen, A. S.; Astakhova, I. V.; Malakhov, A. D.; Babu, B. R.; Korshun, V. A.; Wengel, J. *Bioorg. Med. Chem.* **2008**, *16*, 94–99.

(25) (a) Hrdlicka, P. J.; Kumar, T. S.; Wengel, J. *Chem. Commun.* **2005**, 4279–4281. (b) Kumar, T. S.; Wengel, J.; Hrdlicka, P. J. *ChemBioChem* **2007**, *8*, 1122–1125. (c) Andersen, N. K.; Wengel, J.; Hrdlicka, P. J. *Nucleosides Nucleotides Nucleic Acids* **2007**, *26*, 1415–1417. (d) Kumar, T. S.; Madsen, A. S.; Wengel, J.; Hrdlicka, P. J. *Nucleosides Nucleotides Nucleic Acids* **2007**, *26*, 1403–1405.

(26) Preliminary results have been briefly outlined in: Kumar, T. S.; Wengel, J.; Hrdlicka, P. J. *Nucleosides Nucleotides Nucleic Acids* **2007**, *26*, 1407–1409.

SCHEME 1. Structures of α-L-LNA (O), Abasic (Φ), 2′-Amino-α-L-LNA (X), and 2′-*N*-(Pyren-1-yl)acetyl-2′-amino-α-L-LNA (Y) Monomers (*T* = thymin-1-yl; Py = pyren-1-yl)

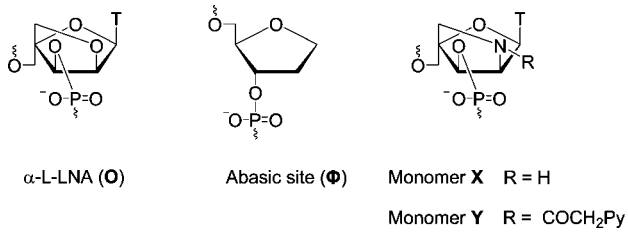

conventional procedures except for extended coupling times (10 min using 1*H*-tetrazole as catalyst). Composition and purity (>80%) of all modified ONs was confirmed by MALDI-MS (Table S3 in the Supporting Information) and ion exchange HPLC, respectively.[27]

Initial Thermal Denaturation Studies. The effect upon incorporation of monomers **O**, **X**, or **Y** into ONs on thermal affinity toward complementary DNA or target strands containing abasic monomer **Φ** (subsequently termed *abasic target strands*) was evaluated by UV thermal denaturation experiments using medium salt buffer conditions ($[Na^+] = 110$ mM).[27] Denaturation curves of all modified duplexes with a reported T_m value exhibited sigmoidal monophasic transitions with similar shapes as observed for unmodified reference duplexes (Figure S1 in the Supporting Information).[27]

In agreement with literature, a single incorporation of these monomers in a central position of a 9-mer mixed sequence ON increased thermal affinity toward DNA complements relative to the unmodified reference strand (Table 1), in the following order: monomer **Y**[25b] > **O**[20,28] > **X**.[22] The pronounced increase in duplex stability induced by monomer **Y** ($\Delta T_m = +15.5$ °C, compare T_m values of **ON4**:**ON5** and **ON1**:**ON5**, Table 1) is particularly noteworthy and has been attributed to intercalation of the pyrene moiety.[25b]

Interestingly, pyrene-functionalized monomer **Y** induced even more pronounced stability-enhancing effects in duplexes with target strands containing abasic monomer **Φ** in a *+1 interstrand position* relative to monomer **Y**; that is, **ON4**:**ON8** exhibited an increase in T_m value of more than +18.5 °C relative to the corresponding reference duplex **ON1**:**ON8** (Table 1), thus comparing favorably with state-of-art probes.[3a,4c,14] Duplex formation between abasic target strands **ON6**−**ON8** and unmodified strand **ON1**, α-L-LNA **ON2**, or 2′-amino-α-L-LNA **ON3** was not observed (T_m <10 °C, Table 1). The remarkable stabilization of abasic sites in +1 interstrand positions by 2′-*N*-(pyren-1-yl)acetyl-2′-amino-α-L-LNA [we define 2′-*N*-(pyren-1-yl)acetyl-2′-amino-α-L-LNA as an oligonucleotide containing one or more 2′-*N*-(pyren-1-yl)acetyl-2′-amino-2′-deoxy-2′-*N*,4′-*C*-methylene-α-L-ribofuranosyl monomer(s)] may also be illustrated by comparing T_m values between duplexes with complementary DNA strands (e.g., **ON4**:**ON5**) and with abasic target strands (e.g., **ON4**:**ON8**). While introduction of an abasic site resulted in decreases of T_m values of more than 18.5−24.5 °C with unmodified DNA, α-L-LNA, or 2′-amino-α-L-LNA, merely a 15.5 °C decrease was observed with pyrene-functionalized 2′-amino-α-L-LNA **ON4** (Table 1). These data strongly suggest that stabilization of abasic sites in +1 interstrand positions by 2′-*N*-(pyren-1-yl)acetyl-2′-amino-α-L-LNA is a result of the appended pyrene moiety rather than direct conformational effects of the bicyclic α-L-LNA skeleton. Lowest energy structures from molecular modeling of **ON4**:**ON7** and **ON4**:**ON8** (Figures S3 and S2 in the Supporting Information, respectively) along with thermodynamic parameters obtained via melting curve analysis (Table S5 in the Supporting Information) provide additional support for this hypothesis. The reader is directed to the Supporting Information for further discussion.[27]

Duplexes with YΦ:AΦ Arrangements—Unprecedented Stabilization of Abasic Sites. The pronounced stabilization of abasic site target strands by 2′-*N*-(pyren-1-yl)acetyl-2′-amino-α-L-LNA triggered us to investigate if introduction of additional abasic sites into duplexes in the vicinity of monomer **Y** could be tolerated. Accordingly, **ON9**, having an incorporation of monomer **Y** flanked on the 3′-side by an abasic site **Φ** (i.e., **YΦ** unit), was prepared and hybridized to abasic target strand **ON8** to give a duplex featuring a **YΦ**:**AΦ** unit. This duplex **ON9**:**ON8** was found to *further increase* duplex stability by 14.5 °C compared to the corresponding duplex with a **YA**:**AΦ** unit (compare T_m values for **ON9**:**ON8** and **ON4**:**ON8**, Tables 2 and 1, respectively). Even more remarkably, **ON9**:**ON8** was as stable as **ON4**:**ON5** with a **YA**:**AT** unit, that is, the corresponding duplex with an intact A:T pair instead of an abasic:abasic pair. Thus, **ON9** containing *a single* **YΦ** *unit stabilizes its abasic target strand* **ON8** by more than 33.0 °C relative to the unmodified 9-mer **ON1**. *Increases in hybridization affinity of this magnitude toward abasic target strands are unprecedented*.

Lowest energy structures from molecular modeling of **ON9**:**ON8** suggest that the pyrene moiety of monomer **Y** occupies the void formed by the two abasic sites whereby interruption of base stacking in the central duplex region is compensated extraordinarily well and a continuous $\pi-\pi$ stacking is ensured (Figure S4 in the Supporting Information).[27] For additional discussion, the reader is referred to the Supporting Information.[27] The proposed intercalation of the pyrene moiety of **ON9**:**ON8** is further corroborated by the biophysical properties of the corresponding 13-mer duplexes with multiple **YΦ** units, which include bathochromic shifts and increased CD signals from the pyrene moieties of monomer **Y**, and favorable entropic contributions to stabilization, all of which suggest intercalation of the pyrene unit (vide infra). Our studies therefore indicate that the **YΦ** unit positions the pyrene moiety in a similar *structural environment* as observed with the pyrene nucleosides developed in the Kool group,[3a,13] yet even more pronounced stabilization of abasic sites is observed.

Duplexes with YΦ:AB Arrangements—Universal Base Behavior and Base Flipping. Interestingly, replacement of abasic monomer **Φ** by a natural deoxyribonucleotide in the "bottom" strand (**ON10**−**ON13**) did not change the thermal stability of duplexes with **ON9** noticeably (Table 2). Universal base behavior has also been reported for related LNA and α-L-LNA analogues where a pyrene moiety replaced the nucleobase,[4] but substantially higher hybridization affinities toward target strands are observed with the present **YΦ** probes, which again are rationalized by energetically favorable entropy effects as outlined above. Molecular modeling of **ON9**:**ON13** (**YΦ**:**AT** arrangement) suggests that intercalation of the pyrene moiety results in an unstacking of the base moiety of **T13** into the major groove (opposite of **Φ**, see Figure S5 in the Supporting

(27) See Supporting Information.
(28) (a) Rajwanshi, V. K.; Håkansson, A. E.; Dahl, B. M.; Wengel, J. *Chem. Commun.* **1999**, 1395–1396. (b) Rajwanshi, V. K.; Håkansson, A. E.; Kumar, R.; Wengel, J. *Chem. Commun.* **1999**, 2073–2074.

TABLE 1. Thermal Denaturation Temperatures of Duplexes between 5′-GTG ABA TGC and DNA Complements or Target Strands Containing an Abasic Site at Different Interstrand Zipper Positions (ON5−ON8)[a]

			T_m[a] (°C)			
			5′-GTG A**B**A TGC			
		Description	**ON1**, **B** = T	**ON2**, **B** = **O**	**ON3**, **B** = **X**	**ON4**, **B** = **Y**
ON5	3′-CAC TAT ACG	Complement	28.5	34.5	29.0[b]	44.0
ON6	3′-CAC **Φ**AT ACG	−1 position	<10 °C	<10 °C	<10 °C	16.5
ON7[c]	3′-CAC T**Φ**T ACG	0 position	<10 °C	<10 °C	<10 °C	15.0
ON8	3′-CAC TA**Φ** ACG	+1 position	<10 °C	<10 °C	<10 °C	28.5

[a] Thermal denaturation temperatures [T_m values/°C] measured as the maximum of the first derivative of the melting curve (A_{260} vs temperature) recorded in medium salt buffer ([Na^+] = 110 mM, [Cl^-] = 100 mM, pH 7.0 (NaH_2PO_4/Na_2HPO_4)), using 1.0 μM concentrations of the two complementary strands. T_m values are averages of at least two measurements; A = adenin-9-yl DNA monomer, C = cytosin-1-yl DNA monomer, G = guanin-9-yl DNA monomer, T = thymin-1-yl DNA monomer. See Scheme 1 for structure of monomers **O**, **X**, **Y**, and **Φ**. [b] See ref 22. [c] See ref 4c.

TABLE 2. Thermal Denaturation Temperatures of Duplexes between ON9 (5′-GTG AYΦ** TGC) and Target ON Strands ON8 or ON10−ON13[a]**

		T_m[a] (°C)				
		3′-CAC TA**B** ACG				
		ON8, **B** = **Φ**	**ON10**, **B** = A	**ON11**, **B** = C	**ON12**, **B** = G	**ON13**, **B** = T
ON9	5′-GTG A**Y**Φ TGC	43.0	40.0	41.5	44.0	42.5

[a] For conditions of thermal denaturation experiments, see legend of Table 1. See Scheme 1 for structure of monomer **Y** and **Φ**.

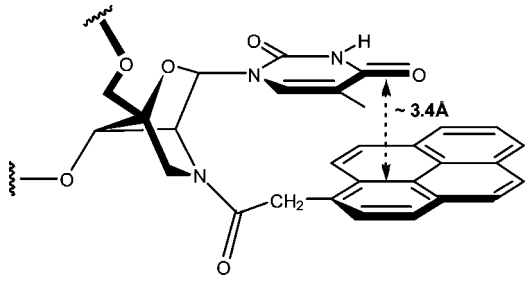

FIGURE 1. Preorganization between the nucleobase and pyrene moiety of monomer **Y** as indicated from molecular modeling (see Supporting Information).

Information). For additional discussion, the reader is referred to the Supporting Information.[27] A base flipping mechanism is in agreement with the observed lack of thermal preference for nucleotides opposite of abasic monomer **Φ** of **ON9** and the observation that very similar steady-state fluorescence spectra were observed for duplexes between **ON9** and **ON8** or **ON10**−**ON13** (results not shown), suggesting that the pyrene moiety is in similar positions in all cases. Base flipping mechanisms have previously been suggested for probes modified with pyrene nucleotides[29,30] or nucleotides with Watson−Crick base pair mimics.[14]

The highly interesting properties of duplexes with incorporations of monomer **Y** prompted us to further consider the basis of its stabilizing effects. On the basis of molecular modeling studies (see Supporting Information), the relative molecular arrangement between the 2-oxo-5-azabicyclo[2.2.1]heptane skeleton, the short acetyl linker, and the nucleobase and pyrene moieties of monomer **Y** can be schematically illustrated as shown in Figure 1. The bicyclic skeleton efficiently locks the relative positions of C1′ and N2′ whereto the nucleobase and pyrene moieties are attached. Moreover, since the glycosidic torsion angle of α-L-LNA type nucleotides preferably adopts *anti* conformations and a short rigid amide linker is used to attach the pyrene moiety to the bicyclic skeleton, the thymine:adenine base pair and the pyrene moiety are forced (preorganized) to adopt an interplanar distance of ∼3.4 Å (Figure 1). This arrangement should allow very strong Watson−Crick hydrogen bonding (via thymine) as well as very efficient $\pi-\pi$ stacking (via pyrene) with the complementary adenine or with neighboring bases.

Duplexes with High Content of Abasic Sites—Probing Limits of Duplex Integrity. DNA duplexes containing multiple **YΦ**:**AΦ** units were constructed to estimate the upper tolerable content of abasic sites in duplexes with respect to maintaining structural integrity. 13-Mer ONs containing two or four **YΦ** units, positioned either consecutively or separated by a single nucleotide (**ON18**−**ON21**), were targeted toward either complementary DNA strands or abasic target strands (**ON15** and **ON17** or **ON22**−**ON25**, Table 3). Duplex **ON20**:**ON24** with two separated **YΦ**:**AΦ** units was considerably more stable than the corresponding unmodified duplex **ON16**:**ON17** (ΔT_m/unit = +6.5 °C), although a less pronounced increase per **YΦ**:**AΦ** unit was observed than in the 9-mer sequence context (ΔT_m/unit = +15.5 °C). In contrast, incorporation of two consecutive **YΦ**:**AΦ** units (**ON18**:**ON22**) resulted in a slight decrease in duplex stability (ΔT_m = −1.0 °C) relative to **ON16**:**ON17**, but still the duplex remained remarkably stable considering the number of abasic sites. These trends were accentuated in duplexes with four **YΦ**:**AΦ** units (i.e., **ON19**:**ON23**), with a contiguous stretch of four **YΦ**:**AΦ** units exhibiting a T_m value of 28.5 °C, while **ON21**:**ON25** with four separated **YΦ**:**AΦ** units formed an *extraordinarily stable duplex with a T_m value of 60.5 °C despite the presence of eight abasic sites distributed over 13 base pairs* (31% content of abasic sites). In comparison, Kool and co-workers have reported formation of stable duplexes containing 20% abasic sites, but did not observe transitions for duplexes with 40% content of abasic sites.[3a] Duplexes with multiple consecutive or separated **YΦ**:**AB** units largely paralleled the behavior of duplexes with **YΦ**:**AΦ** units, although the duplexes in general were slightly less stable (e.g., compare T_m values of **ON20**:**ON17** vs **ON20**:**ON24**, Table 3).

(29) Jiang, Y. L.; Kwon, K.; Stivers, J. T. *J. Biol. Chem.* **2001**, *276*, 42347–42354.
(30) Nakano, S.; Uotani, Y.; Uenishi, K.; Fujii, M.; Sugimoto, N. *J. Am. Chem. Soc.* **2005**, *127*, 518–519.

TABLE 3. Thermal Denaturation Temperatures of Duplexes Containing Multiple Incorporations of YΦ Units[a]

Consecutive **YΦ** units		T_m (ΔT_m/°C)	Separated **YΦ** units		T_m (ΔT_m/°C)
ON14 **ON15**	5′-ACT ATG TAT CTA C 3′-TGA TAC ATA GAT G	35.0	**ON16** **ON17**	5′-CTA GTA ATA GTA C 3′-GAT CAT TAT CAT G	35.0
ON18 **ON15**	5′-ACT A**YΦYΦ**T CTA C 3′-TGA TAC ATA GAT G	28.5 (−6.5)	**ON20** **ON17**	5′-CTA G**YΦ** A**YΦ** GTA C 3′-GAT CAT TAT CAT G	45.0 (+10.0)
ON19 **ON15**	5′-AC**YΦYΦYΦYΦ**TA C 3′-TGA TAC ATA GAT G	nt[b]	**ON21** **ON17**	5′-C**YΦ** G**YΦ** A**YΦ** G**YΦ** C 3′-GAT CAT TAT CAT G	56.0 (+21.0)
ON18 **ON22**	5′-ACT A**YΦYΦ**T CTA C 3′-TGA TA**Φ** A**Φ**A GAT G	34.0 (−1.0)	**ON20** **ON24**	5′-CTA G**YΦ** A**YΦ** GTA C 3′-GAT CA**Φ** TA**Φ** CAT G	48.0 (+13.0)
ON19 **ON23**	5′-AC**YΦYΦYΦYΦ**TA C 3′-TGA **Φ**A**Φ** A**Φ**A **Φ**AT G	28.5 (−6.5)	**ON21** **ON25**	5′-C**YΦ** G**YΦ** A**YΦ** G**YΦ** C 3′-GA**Φ** CA**Φ** TA**Φ** CA**Φ** G	60.5 (+25.5)

[a] For conditions of thermal denaturation experiments, see legend of Table 1, ΔT_m = change in T_m value calculated relative to unmodified reference duplex. See Scheme 1 for structure of monomers **Y** and **Φ**. [b] No clear transition was observed.

TABLE 4. Thermodynamic Parameters Derived from Thermal Denaturation Curves Using van't Hoff Plots

		ΔG^{310} (kJ/mol)	ΔH (kJ/mol)	$T^{310}\Delta S$ (kJ/mol)
ON16 **ON17**	5′-CTA GTA ATA GTA C 3′-GAT CAT TAT CAT G	−35	−345	−310
ON20 **ON17**	5′-CTA G**YΦ** A**YΦ** GTA C 3′-GAT CAT TAT CAT G	−43	−292	−249
ON20 **ON24**	5′-CTA G**YΦ** A**YΦ** GTA C 3′-GAT CA**Φ** TA**Φ** CAT G	−47	−316	−269
ON21 **ON17**	5′-C**YΦ** G**YΦ** A**YΦ** G**YΦ** C 3′-GAT CAT TAT CAT G	−54	−318	−264
ON21 **ON25**	5′-C**YΦ** G**YΦ** A**YΦ** G**YΦ** C 3′-GA**Φ** CA**Φ** TA**Φ** CA**Φ** G	−61	−342	−281
ON14 **ON15**	5′-ACT ATG TAT CTA C 3′-TGA TAC ATA GAT G	−35	−352	−317
ON18 **ON15**	5′-ACT A**YΦ YΦ**T CTA C 3′-TGA TAC ATA GAT G	−29	−292	−263
ON18 **ON22**	5′-ACT A**YΦ YΦ**T CTA C 3′-TGA TA**Φ** A**Φ**A GAT G	−35	−357	−322
ON19 **ON23**	5′-AC**Y ΦYΦ YΦY Φ**TA C 3′-TGA **Φ**A**Φ** A**Φ**A **Φ**AT G	−27	−378	−351

Several biophysical observations suggest intercalation of the pyrene moiety of monomer **Y** as the main contributor to these effects including subtle hybridization-induced bathochromic shifts of pyrene absorption maxima[24e,25a,b,31] ($\Delta\lambda_{max} = 0-3$ nm, Table S4 in the Supporting Information) and slight hybridization-induced increases in circular dichroism signal intensity in the pyrene absorption region between 310 and 370 nm[31] (Figure S7 in the Supporting Information).[27] The reader is directed to the Supporting Information for the full discussion of CD and UV spectra.

In addition, thermodynamic parameters were obtained by melting curve analysis for the studied duplexes assuming bimolecular reactions and two-state equilibria.[32] The markedly increased hybridization affinity of **ON20** (13-mer with two separated **YΦ** units) toward complementary DNA **ON17** relative to the corresponding unmodified reference **ON16** (Table 3) is attributable to a markedly more favorable entropic term ($T\Delta S$(**ON20**:**ON17**) − $T\Delta S$(**ON16**:**ON17**) = +61 kJ/mol), which is largely but not completely counterbalanced by a more unfavorable enthalpic term ($\Delta\Delta H$ = +53 kJ/mol, Table 4). This underlines the hypothesis that the pyrene moiety of monomer **Y** is constructively preorganized (favorable entropy) to intercalate into the void of the duplex core formed in the presence of an abasic site and to thereby partially compensate for the disrupted $\pi-\pi$ stacking (enthalpically unfavorable relative to undisrupted duplex). The *additional increase* in hybridization affinity of **ON20** toward abasic target strand **ON24**, furnishing a duplex with two separated **YΦ**:**AΦ** units, primarily results from improved enthalpic contributions (compare ΔH for **ON20**:**ON24** and **ON20**:**ON17**, Table 4), while entropic components still are more favorable than for the unmodified reference duplex. This suggests a more constructive $\pi-\pi$ stacking between the pyrene moiety and surrounding base pairs in duplexes with two separated **YΦ**:**AΦ** units than **YΦ**:**AT** units. The thermodynamic parameters of the corresponding duplexes between ONs with four separated **YΦ** units and complementary DNA or abasic target strands follow the same general trends as observed with two separated **YΦ** units although they are less pronounced (e.g., compare parameters of **ON21**:**ON17** and **ON20**:**ON17**, Table 4).

Introduction of two *consecutive* **YΦ** units (**ON18**:**ON15**) also results in a more unfavorable enthalpic component ($\Delta\Delta H$ = +60 kJ/mol) relative to the unmodified duplex **ON14**:**ON15**. However, the unfavorable enthalpic component is, unlike **ON20**:**ON17** (two *separated* **YΦ** units), no longer fully compensated by the favorable entropic term ($\Delta(T\Delta S)$ = +54 kJ/mol). Hybridization of **ON18** to abasic target strand **ON22** (two *consecutive* **YΦ**:**AΦ** units) also, like **ON20**:**ON24** (two *separated* **YΦ**:**AΦ** units), results in markedly improved enthalpic contributions relative to **ON18**:**ON15** ($\Delta\Delta H$ = −65 kJ/mol, Table 4). This is to a great extent counteracted by a markedly more unfavorable entropic component. It is noteworthy that the entropic term for **ON18**:**ON22** is even less favorable than for the corresponding unmodified duplex **ON14**:**ON15** ($\Delta(T\Delta S)$ = −5 kJ/mol, Table 4). This trend is even more pronounced in **ON19**:**ON23** (four consecutive **YΦ**:**AΦ** units), where a favorable enthalpy contribution cannot outweigh a very unfavorable entropic component. For a full discussion of the thermodynamic parameters of duplexes listed in Tables 1−3, the reader is directed to the Supporting Information.[27]

Furthermore, molecular dynamics simulations indicate that consecutive **YΦ**:**AΦ** units lead to a markedly higher flexibility of the central segment, when comparing to separated **YΦ**:**AΦ** units (Figures S9 and S10 in the Supporting Information).[27] Additional discussion of results from modeling studies are in Supporting Information.[27]

Collectively, these results demonstrate that consecutive **YΦ**:**AΦ** units are poorly accommodated within DNA duplexes,

(31) Nakamura, M.; Fukunaga, Y.; Sasa, K.; Ohtoshi, Y.; Kanaori, K.; Hayashi, H.; Nakano, H.; Yamana, K. *Nucleic Acids Res.* **2005**, *33*, 5887–5895.
(32) Mergny, J.-L.; Lacroix, L. *Oligonucleotides* **2003**, *13*, 515–537.

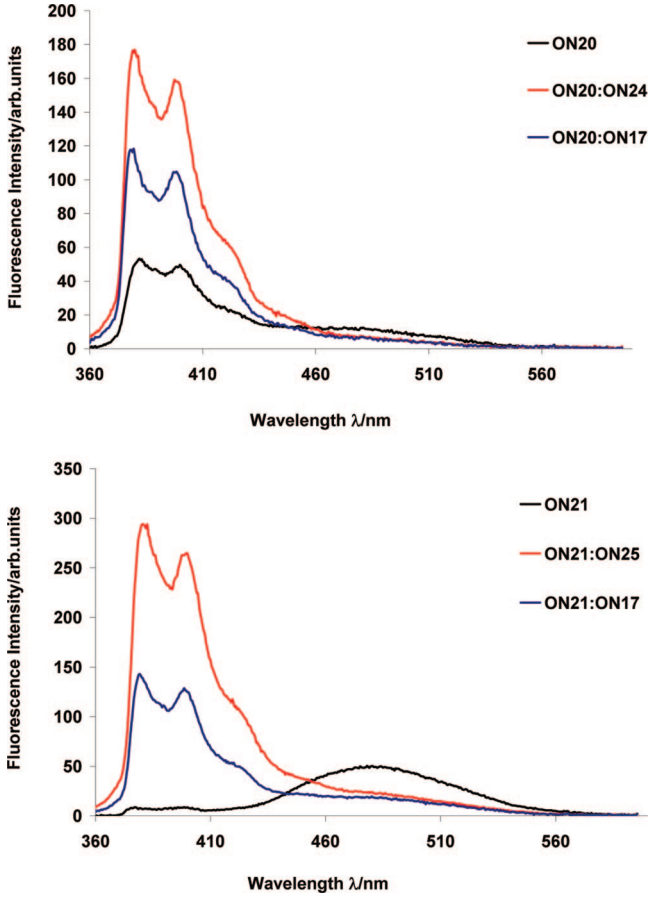

FIGURE 2. Steady-state fluorescence emission spectra. Upper panel: **ON20** (two separated **YΦ** units) and corresponding duplexes with cDNA (**ON17**) or abasic target strand (**ON24**). Lower panel: **ON21** (four separated **YΦ** units) and the corresponding duplexes with complementary DNA (**ON17**) and abasic target strand (**ON25**). Spectra were recorded in thermal denaturation buffer at 5 °C using an excitation wavelength of 350 nm and a concentration of 1.0 μM of each strand.

while separated **YΦ**:**AΦ** units are tolerated very well. It is remarkable that the integrity of **ON21**:**ON25** with an abasic site content of more than 30% not only is maintained but also leads to significantly increased duplex stabilities relative to unmodified DNA duplexes. Interestingly, a similar "nearest neighbor exclusion principle" has been formulated, which states that free intercalators (i.e., noncovalently bound) at most will bind to each second base pair of a DNA duplex due to structural requirements.[33] A direct comparison is, however, complicated by the smaller degree of backbone flexibility, that is, fewer backbone atoms between two intercalators.

Fluorescence Properties of YΦ Probes. Steady-state fluorescence emission spectra were recorded for single-stranded oligonucleotides **ON20** and **ON21** and for the corresponding duplexes with complementary DNA or abasic target strands, using an excitation wavelength of 350 nm (Figure 2). Single-stranded **ON20** (two separated **YΦ** units) exhibited two vibronic bands at 383 and 400 nm (pyrene monomer fluorescence) along with a weak unstructured peak at 480 nm, which normally is attributed to a pyrene−pyrene excimer. Single-stranded **ON21** (four separated **YΦ** units) exhibited a much broader excimer peak. Interestingly, hybridization of **ON20** or **ON21** to abasic target strands results in pronounced increases in fluorescence intensities (~4- and ~16-fold for **ON20** and **ON21**, respectively, measured at approximately 380 nm), while less pronounced increases are observed upon hybridization with DNA complements (Figure 2). Although the molecular mechanism accounting for these observations remains to be elucidated, it is apparent that the self-assembly of these complex architectures can be easily monitored using simple fluorescence assays.

(33) Crothers, D. M. *Biopolymers* **1968**, *6*, 575–584.

Conclusion

Our biophysical studies of duplexes between ONs functionalized with 2′-*N*-(pyren-1-yl)acetyl-2′-amino-α-L-LNA thymine monomer **Y** and abasic target strands (DNA strands containing abasic site monomer **Φ**) have revealed several valuable findings:

(a) 2′-*N*-(Pyren-1-yl)acetyl-2′-amino-α-L-LNA monomers induce *prominent increases in hybridization affinity relative to unmodified ONs toward target strands with abasic sites* in +1 interstrand positions relative to monomer **Y** (**YB**:**AΦ** arrangement). *Stabilization is highly position dependent*.

(b) **YΦ** probes, that is, probes where an abasic monomer **Φ** has been introduced on the 3′-side of monomer **Y**, exhibit even more pronounced increases in hybridization affinity toward abasic target strands (ΔT_m/unit >+33.0 °C relative to the unmodified 9-mer probe strand). *Increases in hybridization affinity of such magnitude toward abasic target strands are unprecedented*.

(c) The conformationally locked 2-oxo-5-azabicyclo-[2.2.1]heptane skeleton of monomer **Y** in concert with the short rigid linker *forces the thymine:adenine base pair and pyrene moiety to adopt an interplanar distance of ~3.4 Å*. The pyrene moiety is, thereby, precisely positioned in the void formed by the **Φ**:**Φ** pair in duplexes containing **YΦ**:**AΦ** arrangements and efficient $\pi-\pi$ stacking is restored. Thus, the **YΦ** unit positions the pyrene moiety in a *similar structural environment as previously reported for nucleosides containing pyrenes as nucleobase surrogate*.[3a,13] Accordingly, a **YΦ** unit can be regarded as a "cousin" to the large family of building blocks with nucleobase surrogates.[2−4,7]

(d) **YΦ** probes exhibit high-affinity universal base behavior, that is, duplexes containing **YΦ**:**AB** units (where **B** = A, C, G, T, or **Φ**) display similar T_m values, which are 11.5−15.5 °C higher than the corresponding fully complementary unmodified DNA duplex. Molecular modeling studies suggest that intercalation of *the pyrene moiety of monomer* **Y** forces the nucleobase moiety of **B** to an extrahelical position. Evaluation of **YΦ** probes as probes inducing base flipping to generate site-selective artificial nucleases,[30] or to elucidate enzymatic mechanisms[2a,29,34−36] is warranted.

(e) Several **YΦ**:**AΦ** units can beneficially be introduced into nucleic acid duplexes if the units are separated by at least one base pair. This allows the construction of *remarkably stable duplexes with a very high content of abasic sites*, for example, the 13-mer *duplex* **ON21**:**ON25** exhibits a T_m *value of 60.5 °C despite the presence of 8 abasic monomers* (ΔT_m = +25.5 °C relative to unmodified duplex). Interestingly, formation of these complex architectures can easily be monitored optically since up to 16-fold increases in fluorescence intensity are observed upon hybridization of **YΦ** probes to abasic target strands.

(34) Sun, L.; Wang, M.; Kool, E. T.; Taylor, J.-S. *Biochemistry* **2000**, *39*, 14603–14610.
(35) Beuck, C.; Singh, I.; Bhattacharya, A.; Hecker, W.; Parmar, V. S.; Seitz, O.; Weinhold, E. *Angew. Chem., Int. Ed.* **2003**, *42*, 3958–3960.
(36) Kwon, K.; Jiang, Y. L.; Stivers, J. T. *Chem. Biol.* **2003**, *10*, 351–359.

Collectively, the data presented herein demonstrate that efficient stacking may offset lack of hydrogen bonding, ascertain structural integrity of nucleic acid duplexes, and lead to the self-assembly of complex nucleic acid architectures, showcasing that chemically modified nucleic acids possess enormous potential for high-density functionalization.[23,37−39] N2′-Functionalized 2′-amino-α-L-LNA monomers stand out in the diverse pool of nucleotide building blocks capable of positioning functional entities in the duplex cores[2−7] by their ability to precisely preorganize aromatic units for intercalation leading to unparalleled increases in thermal duplex stability. We will continue to utilize the inherent characteristics of these building blocks to develop novel diagnostic[25b] and therapeutic[25a] methodologies.

Experimental Section

Synthesis of Modified Oligonucleotides. Syntheses of oligonucleotides (ONs) containing model abasic site (**Φ**), α-L-LNA (**O**), 2′-amino-α-L-LNA (**X**), or 2′-*N*-(pyren-1-yl)acetyl-2′-amino-α-L-LNA (**Y**) monomers (see Scheme 1 for structures) were performed on 0.2 μmol scale using an automated DNA synthesizer. Base-protected deoxynucleotide β-cyanoethyl phosphoramidite monomers (0.05 M dA^{Bz}, dG^{iBu}, dC^{Bz}, and dT in anhydrous CH_3CN) and succinyl-linked LCAA-CPG (long chain alkyl amine controlled pore glass) columns with the pore size of 500 Å were used. Standard procedures were used for unmodified monomers, that is, trichloroacetic acid in CH_2Cl_2 as detritylation reagent; 0.25 M 4,5-dicyanoimidazole (DCI) in CH_3CN as activator; acetic anhydride in THF as cap A solution; *N*-methylimidazole in THF as cap B solution, and 0.02 M iodine in H_2O/pyridine/THF as the oxidizing solution. Unmodified monomers, CPG columns, and all reagents were acquired from commercial sources. Extended coupling times (0.05 M in CH_3CN, 10 min for **Φ**, 15 min for **O**, 30 min for **X** and **Y**) and 1*H*-tetrazole as catalyst were used for the corresponding amidites of the various monomers. The stepwise coupling yields were >99% for unmodified phosphoramidites and >90% for all modified amidites. Removal of nucleobase protecting groups and cleavage from the solid support was achieved using 32% aq ammonia for 12 h at 55 °C. Crude ONs with a dimethoxytrityl group at the O5′ atom (DMT-ONs) were purified by RP-HPLC. The pure fractions were pooled together and detritylated with 80% aq AcOH for 20 min at rt. After detritylation, ONs were precipitated from absolute EtOH (−18 °C, 12 h) and washed with 96% EtOH (2 × 300 μL). ON composition and purity was confirmed MALDI-MS and ion exchange HPLC, respectively.

Protocol for Thermal Denaturation Studies. Concentrations of ONs were estimated using the following extinction coefficients for DNA bases (OD/μmol): G (12.01), A (15.20), T (8.40), C (7.05) and for pyrene (22.4). The two complementary strands (∼1.0 μM of each strand) were thoroughly mixed, and the complex was denatured by heating to 60−90 °C followed by cooling to the starting temperature of the experiment. Quartz optical cells with a path length of 1.0 cm were used. Thermal denaturation temperatures (T_m values/°C) were measured on a UV/vis spectrometer equipped with a Peltier temperature programmer and determined as the maximum of the first derivative of the thermal denaturation curve (A_{260} vs temperature) recorded in medium salt buffer (100 mM NaCl, 0.1 mM EDTA and pH 7.0 adjusted with 10 mM NaH_2PO_4/5 mM Na_2HPO_4). A temperature range from 0−5 to 60−90 °C and a ramp of 1.0 °C/min were used.

Protocol for UV Absorption Measurements. UV absorption measurements were performed on a UV spectrophotometer and quartz optical cells with a path length of 1.0 cm were used. Measurements were conducted using 1.0 μM of strands in T_m buffer. Corrections were made for solvent background, and solutions were heated to 60−90 °C prior to measurements followed by cooling to the starting temperature. UV absorption spectra (200−500 nm) were recorded.

Protocol for Steady-State Fluorescence Measurements. Fluorescence measurements were performed on a luminescence spectrometer equipped with a temperature controller. Quartz optical cells with a path length of 1.0 cm were used. Measurements were conducted using 1.0 μM of strands in T_m buffer. Corrections were made for solvent background, but no attempts were made to eliminate dissolved oxygen in the buffer solution. Solutions were heated to 60−90 °C prior to measurements followed by cooling to the starting temperature. Steady-state fluorescence emission spectra (360−600 nm) were recorded at 5 °C (±0.1 °C) as an average of five scans at an excitation wavelength of 350 nm using an excitation slit of 4.0 nm, emission slit of 2.5 nm, and scan speed of 120 nm/min.

Protocol for Circular Dichroism Studies. Circular dichroism (CD) spectra were recorded on a CD spectrometer using quartz optical cells with a 5 mm path length. Measurements were conducted using 4.0 μM of strands in T_m buffer. Corrections were made for buffer background, and solutions were heated to 60−90 °C prior to measurements followed by cooling to the starting temperature. CD spectra (200−600 nm) were recorded at 5 °C (±0.1 °C) as an average of five scans and with a scan speed of 100 nm/min.

Acknowledgment. The Nucleic Acid Center at the University of Southern Denmark is funded by the Danish National Research Foundation for studies on nucleic acid chemical biology. We greatly appreciate funding from the Danish National Research Foundation, the Oticon Foundation, Idaho NSF EPSCoR (Experimental Program to Stimulate Competitive Research), BANTech Center at Univ. of Idaho, and the Student Grants Program at Univ. of Idaho. The Ph.D. school Nucleic Acid Based Drug Design (NAC DRUG) supported by the Danish Agency for Science Technology and Innovation is gratefully acknowledged.

Supporting Information Available: Protocols for preparative RP-HPLC (purification, Table S1) and ion-exchange HPLC (purity analysis, Table S2); MALDI-MS data of ONs (Table S3); representative thermal denaturation curves for **ON16**:**ON17** and **ON21**:**ON25** (Figure S1); molecular modeling discussion of 9-mer duplexes **ON4**:**ON8**, **ON4**:**ON7**, **ON9**:**ON8**, and **ON9**:**ON13**; energy minimized structures of **ON4**:**ON8** (Figure S2); energy minimized structures of **ON4**:**ON7** (Figure S3); energy minimized structures of **ON9**:**ON8** (Figure S4); energy minimized structures of **ON9**:**ON13** (Figure S5); overlay of structures from MD simulation of **ON4**:**ON7**, **ON4**:**ON8**, **ON9**:**ON8**, and **ON9**:**ON13** (Figure S6); absorption maxima of single-stranded probes and duplexes containing multiple of **YΦ** units (Table S4); CD spectra and additional discussion thereof for strands/duplexes involving **ON14**−**ON21** (Figure S7); thermodynamic parameters for both 9-mer and 13-mer duplexes and additional discussion thereof (Table S5); molecular modeling discussion of 13-mer duplexes; energy minimized structures of **ON18**:**ON22** (two consecutive **YΦ**:**AΦ** units) and **ON20**:**ON24** (two separate **YΦ**:**AΦ** units) (Figure S8); plots depicting phase angle variation as a function of simulation time for **ON18**:**ON22** and **ON20**:**ON24** (Figure S9 and S10); overlay of structures from MD simulation of **ON18**:**ON22** and **ON20**:**ON24** (Figure S11); molecular modeling protocol. This material is available free of charge via the Internet at http://pubs.acs.org.

JO800551J

(37) Benvin, A. L.; Creeger, Y.; Fisher, G. W.; Ballou, B.; Wagonner, A. S.; Armitage, B. A. *J. Am. Chem. Soc.* **2007**, *129*, 2025–2034.

(38) Benvin, A. L.; Creeger, Y.; Fisher, G. W.; Ballou, B.; Wagonner, A. S.; Armitage, B. A. *J. Am. Chem. Soc.* **2007**, *129*, 2025–2034.

(39) Persil, Ö.; Hud, N. V. *Trends Biotechnol.* **2007**, *25*, 433–436.